

NACA RM L56G20

7712

~~CONFIDENTIAL~~

HADC

Copy 267  
RM L56G20

TECHNICAL LIBRARY

APR 28 1957

001 1 251

014184



TECH LIBRARY KAFB, NM



# RESEARCH MEMORANDUM

EXPERIMENTAL HINGE MOMENTS ON FREELY OSCILLATING  
FLAP-TYPE CONTROL SURFACES

By C. William Martz

Langley Aeronautical Laboratory  
Langley Field, Va.

~~CONFIDENTIAL~~  
...of the espionage laws, Title 18, U.S.C., Secs. 793 and 794, the transmission or revelation of which in any unauthorized person is prohibited by law.

## NATIONAL ADVISORY COMMITTEE FOR AERONAUTICS

WASHINGTON  
October 12, 1956

~~CONFIDENTIAL~~



## NATIONAL ADVISORY COMMITTEE FOR AERONAUTICS

## RESEARCH MEMORANDUM

EXPERIMENTAL HINGE MOMENTS ON FREELY OSCILLATING  
FLAP-TYPE CONTROL SURFACES

By C. William Martz

## SUMMARY

Oscillatory hinge-moment characteristics have been obtained from free-flight tests of two rocket-powered models each equipped with a 60° sweptback clipped delta wing featuring an unbalanced, constant-chord, full-span trailing-edge control. One control had a sharp trailing edge, and the other had a trailing-edge thickness equal to 1/2 the thickness at the hinge line. Data were obtained at zero angle of attack and control reduced frequencies ranged from 0.09 to 0.035. The Mach number range of the investigation was from 0.4 to 1.9.

Results indicate that except for a region of mild instability between the Mach numbers of 0.75 and 0.9, aerodynamic control damping was stable up to near sonic velocities where control-surface flutter developed for both models. For the blunt-trailing-edge control, this instability continued to a Mach number of at least 1.3. Aerodynamic control damping was found to be very sensitive to amplitude of oscillation at transonic speeds.

Aerodynamic control-restoring moments were stable throughout the Mach range for both controls. Increasing the control trailing-edge thickness had little effect on control damping moments but increased the stability of the control restoring moments an average of 12 percent at supersonic speeds and 35 percent at subsonic speeds.

## INTRODUCTION

One of the troublesome features of the transonic and lower supersonic speed ranges is the phenomenon of single degree-of-freedom control-surface flutter or control buzz as it is referred to sometimes. Although the existence of this torsional instability is predicted by two-dimensional potential flow theory (refs. 1 and 2), there is experimental indication that shock separated flow also may have an important effect

(refs. 3 and 4). Some of the more recent investigations concerning this problem can be found in references 5 to 9.

In an effort to obtain additional experimental information relating to this problem, a rocket model investigation employing the free oscillation technique was conducted to measure the oscillatory hinge moments at zero angle of attack of two trailing-edge controls on a  $60^\circ$  sweptback delta wing for Mach numbers between 0.4 and 1.9. Reynolds number based on the wing mean aerodynamic chord varied from  $3.5 \times 10^6$  to  $19 \times 10^6$ . Control reduced frequencies ranged from 0.09 to 0.035. Data were obtained at control oscillation amplitudes between  $\pm 1^\circ$  and  $\pm 3^\circ$  at subsonic speeds. At supersonic speeds some data were obtained both at low amplitudes ( $\pm \frac{1^\circ}{2}$ ) and at high amplitudes ( $\pm 3^\circ$  to  $\pm 14^\circ$ ).

Results are presented herein and are compared with potential flow theory and tunnel test results.

Preliminary results of one of the present test flights have been presented previously in reference 7.

#### SYMBOLS

c	control chord, ft
V	free-stream velocity, ft/sec
M	Mach number
q	free-stream dynamic pressure, lb/sq ft
R	Reynolds number based on wing mean geometric chord of 1.486 ft
$M_\delta$	aerodynamic control hinge moment per unit deflection, ft-lb/radians
$C_h$	control hinge-moment coefficient, $\frac{\text{Control hinge moment}}{2M^2q}$
$\delta$	control-surface deflection, positive trailing edge down, radians except as noted
$\dot{\delta}$	time derivative of control-surface deflection, radians/sec

$C_{h\delta,\omega}$	control restoring moment coefficient, $\frac{\text{Real part of } M_{\delta}}{2M'q}$ per radian
$C_{h\delta^*,\omega}$	control damping moment coefficient, $\frac{\text{Imaginary part of } M_{\delta}}{2M'qk}$ per radian
$\omega$	control damped natural frequency, radians/sec
$\omega_0$	control damped natural frequency in still air, radians/sec
$k$	control reduced frequency, $\frac{\omega c}{2V}$
$M'$	moment of control area rearward of and about hinge line, cu ft
$L$	control span, ft
$\bar{M}_3$	flutter derivative, $-C_{h\delta,\omega} \frac{M'}{c^2 k^2 L}$ (see ref. 2)
$\bar{M}_4$	flutter derivative, $-C_{h\delta^*,\omega} \frac{M'}{c^2 k L}$ (see ref. 2)
$a_z$	model longitudinal acceleration, ft/sec <sup>2</sup> .

In stability notation, the symbols  $C_{h\delta,\omega}$  and  $C_{h\delta^*,\omega}$  are defined as follows:

$$C_{h\delta,\omega} = \frac{\partial C_h}{\partial \delta}$$

$$C_{h\delta^*,\omega} = \frac{\partial C_h}{\partial \frac{\delta c}{2V}}$$

## MODELS AND TESTS

## Models

The models used in this investigation consisted of a pointed cylindrical fuselage equipped with  $60^\circ$  sweptback clipped delta wings. Vertical tail fins provided yaw stability. The models were identical except for the control plucking system and control-surface section. The fuselage consisted of a fabricated aluminum-alloy core wrapped with mahogany. The nose cone was plastic and the tail section was a magnesium tube. A sketch of the models showing dimensions is presented in figure 1 and photographs of the models are shown in figure 2.

The wings were of solid magnesium alloy and had an NACA 65A005 airfoil section. The right wing panel embodied a constant-chord (13 percent exposed wing root chord), full-span, trailing-edge control. The control was hinged at its leading edge through a cantilever-type flexure hinge. The spanwise distribution of flexure hinge and, hence, extent of sealed gap can be seen for model A in figure 2(c). The region of sealed gap for model B extended over the entire control span except for the outboard 10 percent. An auxiliary pin-type hinge was located inboard the fuselage to restrict translation of the flexure hinge at the inboard end. (See fig. 3.)

The controls were made of steel and had a modified wedge section. The control of model A had a sharp trailing edge, and the control trailing-edge thickness of model B was one-half that of the hinge line thickness. See figure 1 for control section.

Experimentally determined dynamical constants of both models are presented in table I.

## Flight Tests

The flight tests were conducted at the Langley Pilotless Aircraft Research Station at Wallops Island, Va. Both models were boosted to a Mach number of about 1.9 and coasted back down the Mach number range. The control plucking systems were started just before launching and most of the usable data were obtained during the boosted portion of the flights when the models were being accelerated longitudinally from 24 to 30 times the acceleration of gravity.

Existing flight conditions resulted in the values of Reynolds number and dynamic pressure presented in figures 4 and 5 as a function of Mach number.

## INSTRUMENTATION

Inductance-type instruments measured time histories of control deflection, total pressure, and normal acceleration of both wing panels. These data were telemetered to a ground receiving station and recorded. Response of the measuring and recording instrumentation was such as to require no correction to the recorded data at the frequencies encountered in the tests.

A radiosonde was used to obtain atmospheric data at all flight altitudes. Flight-path data were obtained from SCR-584 tracking radar, and CW Doppler radar was used to determine initial flight velocity and longitudinal acceleration.

## TECHNIQUE

The free oscillation technique was used in this investigation. The controls were plucked periodically by means of a motor driven cam (see figure 3 for sketch of control plucking system) and the resultant free oscillations of the control were recorded as shown in figure 6. With the assumptions that the control motion was effectively restricted to one degree of freedom and that the aerodynamic damping forces on the control could be represented adequately by viscous forces, the in-phase or restoring component of the control hinge moments was obtained from the frequency of the control oscillation and the control out-of-phase or damping component was determined from the rate of logarithmic growth or decay of the oscillation. The procedure used in reducing the data to obtain the aerodynamic hinge-moment coefficients is presented in the appendix.

The frequency of the plucking action for models A and B was 3 cps and 5 cps, respectively. The amplitude at which the controls of models A and B were released at the end of their respective plucking actions was  $3.0^\circ$  and  $3.5^\circ$ .

## CORRECTIONS

## Wing Effects

Evidence that the wings were oscillating in flight was obtained through the use of wing vibrometers located as shown in figure 1. Figure 6 shows a portion of the time history of the wing vibrometer traces for both models. These oscillations can be seen to consist of a fundamental frequency equal to the control frequency and one or more

harmonics. Thus, it is concluded that the control was exciting the wing by means of inertial and aerodynamic loads. It should be mentioned that the amplitude of these wing oscillations was small (not more than  $\pm 0.03$  inch at the vibrometers) throughout the flights.

Concerning the inertial effects of the wing motion on control restoring moments, an expression relating the coupled frequency of an undamped two-degree-of-freedom system (wing first bending and control rotation modes) with the control natural frequency was obtained as a function of two ratios: the ratio of wing first bending frequency to control natural frequency and the ratio of control inertia about the hinge line to the wing first bending inertia. Using this expression with a calculated inertia ratio of 0.066 and a frequency ratio of 2 resulted in a change in control frequency of 1 percent. This change in frequency is about a maximum for the investigation and indicates the inertial effect of wing motion on the control restoring moment to be about 2 percent or less.

The author was unable to justify the damping-moment data in the aforementioned manner. However, some indication that the control motion was effectively single degree of freedom at low frequencies can be obtained from the clean-looking still-air response of model A control to a step input as presented in figure 6(c). Also, at flight frequencies (see figs. 6(a) and 6(b)), there are no apparent effects of the wing motion on the control trace although it would be expected that the higher frequency components of the wing motions would appear on the control trace if strong coupling of the motions were present.

In view of the preceding remarks, it is believed that the effect of the wing motion on the test results probably is small.

#### Acceleration Effects

Most of the data obtained in this investigation were measured during a condition of high longitudinal acceleration (24 to 30 times the acceleration of gravity). Appropriate corrections for the inertial effects of these accelerations were applied to the data as shown in the appendix. No corrections were applied to the data for any aerodynamic effects of this acceleration.

It should be mentioned that the effect of rocket motor vibrations on the test results was investigated and found to be negligible both for the restoring-moment data and the damping-moment data.

~~CONFIDENTIAL~~

### ACCURACY

The following probable errors have been estimated for the results of the investigation. In the present usage, probable error is the value that any given error will as likely fall under as exceed.

Mach number	Error in $C_{h\delta}$	Error in $C_{h\delta}$	
		$a_2(+)$	$a_2(-)$
0.5	$\pm 1\frac{1}{2}$	$\pm 0.11$	-----
.74	$\pm \frac{3}{4}$	$\pm .07$	-----
.96	$\pm \frac{1}{2}$	$\pm .05$	-----
1.02	$\pm \frac{3}{4}$	$\pm .10$	$\pm 0.17$
1.85	---	$\pm .04$	$\pm .06$

### RESULTS AND DISCUSSION

#### Control Pulsing Systems

The control plucking system, designed originally as shown in figure 3(b), was intended to pluck the control surface periodically and to avoid the possibility of jamming. Since certain of the assumptions used in calculating the motions and loads of the cam and control surface during the plucking action were questionable, an attempt was made to simulate flight loads on the plucking system of the completed model. This was accomplished by mounting the model on an electrodynamic shaker and resonantly vibrating the control to an amplitude of about  $\pm 7^\circ$ , at which time the plucking system was turned on. (The control amplitude of  $\pm 7^\circ$  represented the maximum that could be obtained with the equipment and type of mounting used.) This test was repeated several times without damaging the plucking mechanism, so the system was considered ready for flight testing.

During the flight test (model B), the system worked as planned until control buzz was encountered. The control oscillation quickly built up to an amplitude of about  $\pm 14^\circ$ , shortly after which the impact of the

~~CONFIDENTIAL~~

control surface on the cam caused shear failure of the pin connecting the worm gear and cam shaft. Although data were obtained before and, to a limited extent, even after this failure (the latter due to a slight catching action of the broken pin as it rotated by its broken ends), the plucking system was useless during buzz. As a result of this test the system was redesigned for use with model A as shown in figure 3(a).

The second design incorporated two important features lacking in the previous design: the contact between the cam and control was made gradual instead of abrupt and a means of absorbing vibrational energy was provided by a rubber coupling between the cam drum and worm gear (see fig. 3(a)). This system was flight tested in model A and performed satisfactorily throughout the entire flight which included regions of control buzz. However, during the initial occurrence of buzz, the control position instrument failed and subsequent control data had to be obtained from the wing vibrometers as explained in the appendix.

#### Control Damping

The aerodynamic control damping coefficient  $C_{h\delta, \omega}$  is presented in figure 7 as a function of Mach number for both models. Negative values indicate a stable damping influence of the airstream on the control. The relationship of  $C_{h\delta, \omega}$  with a similar parameter in flutter notation,  $\bar{M}_4$ , is given in the section entitled "Symbols."

Shown for comparison in figure 7 are tunnel-test results for a control similar to that of model A and theoretical values extracted from references 1 and 6 for a ratio of flap chord to wing chord of 0.195. Since the theory of reference 6 was not computed for Mach numbers greater than 0.8, the curve was interpolated between  $M = 0.8$  and the sonic value from reference 1. All theoretical values were determined for the same values of reduced-frequency parameter as existed in the present investigation and which are presented in figure 8 as a function of Mach number.

The curves of figure 7 show stable values of aerodynamic damping up to about  $M = 0.75$  for the sharp-trailing-edge control with a region of mild instability extending to about  $M = 0.9$ . A more severe loss of stability started at  $M = 0.99$  where the damping abruptly became unstable with a slight increase in Mach number and the control oscillation quickly increased in amplitude to about  $\pm 11^\circ$ , the aerodynamic control damping becoming less unstable as control amplitude increased. At the amplitude of about  $\pm 11^\circ$ , the unstable damping of the airstream was balanced by the structural damping of the control system to produce a limited amplitude oscillation. It was during the next plucking action ( $M = 1.12$ ) that

failure of the control position instrument occurred. This failure prevented further control damping measurements.

The damping curve for the blunt-trailing-edge control is seen to be similar to that of the sharp-trailing-edge control. Although it might be stated that the blunted control exhibits more aerodynamic stability over most of the Mach number range presented, the difference is small and deserves no emphasis. As before, aerodynamic control damping abruptly became unstable at near sonic speeds and its nonlinear variation with oscillation amplitude resulted in a limited amplitude oscillation of about  $\pm 14^\circ$ . It was shortly after this time in the flight that the plucking system became damaged. The control continued to oscillate at nearly constant amplitude until a Mach number of 1.3 was obtained at which time the amplitude of the control oscillation started to decrease. Because of the nature of the plucking system failure, no quantitative damping data were obtained beyond  $M = 1.04$  although it is known that the aerodynamic damping was unstable up to  $M = 1.3$ .

Comparison of the sharp-trailing-edge data with the experimental values of reference 8 is poor, and consideration of the effects of reduced frequency does not improve the comparison. Although the theory does not predict the shape of the experimental curves at high subsonic speeds and differs widely with some of the measured values, it does predict the most important feature of the curves, the severe loss of stable damping at near sonic speeds.

It has been pointed out to the author that possibly the poor comparison of the damping values with theory in the Mach number range up to 0.90 could be the result of flow disturbances at the inboard ends of the controls caused by a part of the plucking mechanisms extending beyond the fuselage. (See figs. 2(b) and 2(c).) Also a possibility is the fact that these data were obtained under a condition of high longitudinal acceleration (24 to 30 times the acceleration of gravity), the aerodynamic effects of which are unknown.

#### Control Restoring Moments

The aerodynamic in-phase or restoring moment coefficient  $C_{h\delta, \omega}$  is presented in figure 9 as a function of Mach number for both controls investigated. Since the variation of restoring-moment coefficient with deflection may be nonlinear, these values should be considered as average or effective values for the deflection ranges tested. Shown for comparison are the tunnel data of reference 8 for a control similar to that of model A and potential flow theory from references 1, 2, and 6 which was computed for the reduced frequencies obtained in the present test. The relationship of  $C_{h\delta, \omega}$  with a similar parameter in flutter terminology  $\bar{M}_3$  is given in the section entitled "Symbols."

Aerodynamic control restoring moments were stable throughout the Mach number range for both models.

The flagged data of model B were obtained at small amplitudes of control oscillation (about  $\pm 1\frac{1}{2}^\circ$ ) during decelerated flight and were not faired with the accelerated flight data which were obtained at control oscillation amplitudes up to  $\pm 14^\circ$  at supersonic speeds and from  $\pm 1^\circ$  to  $\pm 3^\circ$  at subsonic speeds. Although the small deflection data contain sizeable errors because of the limited number of cycles that were available for determining control frequency, one effect of the small amplitudes clearly appears to be a substantial increase in control restoring-moment coefficient at transonic speeds.

Increasing the ratio of control trailing-edge thickness to thickness at the hinge line from 0.1 (model A) to 0.5 (model B) is seen to increase the magnitude of the control restoring moments an average of about 35 percent at subsonic speeds and 12 percent at supersonic speeds. This result is in qualitative agreement with other test results (see refs. 9 and 10).

The experimental data of reference 8 are seen to be in fair agreement with model A values at supersonic speeds. However, this comparison is poor at subsonic speeds and no explanations are apparent to the author. It might be mentioned that, according to the theory of reference 6, the effect of any reasonable difference in reduced-frequency parameter would account for only about 10 to 15 percent of this disagreement. Similarly, the supersonic potential flow theory, which includes effects of control aspect ratio, is in good agreement with measured results, whereas the subsonic theory of reference 6 predicts a much more negative result than was obtained in the present tests.

### CONCLUSIONS

The results of a rocket-powered model investigation between the Mach numbers of 0.4 and 1.9 of the hinge moments on freely oscillating flap-type control surfaces installed at the trailing edge of a  $60^\circ$  delta wing led to the following conclusions:

1. Except for a region of mild instability between the Mach numbers of about 0.75 to 0.9, aerodynamic control damping was stable up to near sonic velocities.
2. At near sonic velocities, control-surface flutter developed for both models and continued, in the case of the half-blunt trailing-edge control, to a Mach number of at least 1.3.

3. Changing the control trailing-edge thickness from sharp to half blunt had little apparent effect on aerodynamic control damping.

4. Aerodynamic control damping was very sensitive to amplitude of oscillation at transonic speeds. The relationship was such as to tend to produce a constant amplitude oscillation.

5. The aerodynamic control restoring moments were stable for both controls throughout the Mach number range. Changing the control trailing-edge thickness from sharp to half blunt increased the magnitude of the control restoring moments about 35 percent at subsonic speeds and 12 percent at supersonic speeds.

Langley Aeronautical Laboratory,  
National Advisory Committee for Aeronautics,  
Langley Field, Va., June 28, 1956.

## APPENDIX

## METHOD OF DATA REDUCTION

The general solution to the single-degree-of-freedom moment equation ( $I\ddot{\delta} + D\dot{\delta} + K\delta = 0$ ) governing the free motion of the control about its hinge axis is the damped sinusoid

$$\delta = A_1 e^{\frac{-Dt}{2I}} \sin(\omega t + \phi)$$

where

- I control mass inertia about the hinge line,  $\frac{K_0}{\omega_0^2}$ , slug-ft<sup>2</sup>
- D torsional damping constant of the system,  $\frac{\text{ft-lb}}{\text{radians/sec}}$
- K torsional spring constant of the system, ft-lb/radian
- $A_1, \phi$  constants dependent upon initial conditions and unimportant to this investigation
- t time, sec
- $\omega$  the control oscillation frequency,  $\sqrt{\frac{K}{I} - \left(\frac{D}{2I}\right)^2}$ , radians/sec
- $\frac{D}{2I}$  the logarithmic damping factor,  $(\log_e A)$ , per sec
- A amplitude of control oscillation envelope
- ( $\dot{\quad}$ ), ( $\ddot{\quad}$ ) indicate first and second order time derivatives, respectively

Subscripts o refer to preflight values measured in still air

Thus, by measuring the frequency and logarithmic damping factor of the control oscillation, values of D and K can be calculated knowing the control inertia. These values include both structural and aerodynamic terms. The following relationships were used to extract the aerodynamic coefficients:

~~CONFIDENTIAL~~

For the in-phase or restoring-moment coefficient,

$$\left( \begin{array}{c} \text{Aerodynamic} \\ \text{restoring} \\ \text{moment} \end{array} \right) = \left( \begin{array}{c} \text{Total} \\ \text{restoring} \\ \text{moment} \end{array} \right) - \left( \begin{array}{c} \text{Structural} \\ \text{restoring} \\ \text{moment} \end{array} \right) - \left( \begin{array}{c} \text{Acceleration} \\ \text{restoring} \\ \text{moment} \end{array} \right)$$

or

$$-C_{h_{\delta, \omega}} 2M'q\delta = I \left[ \omega^2 + \left( \frac{D}{2I} \right)^2 \right] \delta - K_0 \delta - a_7 U \sin \delta$$

where  $U$  is the control mass unbalance about the hinge line,  $a_7$  is the model longitudinal acceleration, and  $(\sin \delta)$  is assumed equal to  $\delta$  for the small angles encountered in the investigation. It was found from experience that the effect of damping on the total restoring moment was negligible for the small values of damping obtained in this investigation. Therefore, the final form became:

$$C_{h_{\delta, \omega}} = - \frac{I\omega^2 - K_0 - a_7 U}{2M'q}, \text{ per radian}$$

These values of  $C_{h_{\delta, \omega}}$  are considered average or effective values because of possible aerodynamic nonlinearities.

An extension to the above relation occurred in the reduction of the supersonic data of model A where the instrument measuring control position failed. It was noticed that previous to the failure, the wing vibrometer records had a fundamental frequency equal to the control frequency. By assuming this relationship continued after the failure, it was possible to obtain supersonic  $C_{h_{\delta, \omega}}$  values via the fundamental vibrometer frequency. It is believed that these results would be identical to those obtained from the control oscillation if available.

For damping-moment coefficient,

$$\left( \begin{array}{c} \text{Aerodynamic} \\ \text{damping} \\ \text{moment} \end{array} \right) = \left( \begin{array}{c} \text{Total} \\ \text{damping} \\ \text{moment} \end{array} \right) - \left( \begin{array}{c} \text{Structural} \\ \text{damping} \\ \text{moment} \end{array} \right)$$

or

$$-C_{h_{\dot{\delta}, \omega}} \left( \frac{c}{2V} \right) (2M'q)\dot{\delta} = D\dot{\delta} - D_0 \frac{\omega_0}{\omega} \dot{\delta}$$

The modifying factor  $\frac{\omega_0}{\omega}$  is used in the last term of the previous equation to account for the change in frequency between the preflight still-air measurements of structural damping and the flight measurements of total damping. Its use assumes that structural damping is hysteretic and, unlike viscous damping, is independent of frequency. In final form,

$$C_{h_{\delta},\omega} = - \frac{D - D_0 \frac{\omega_0}{\omega}}{\frac{c}{2V} 2M'q}, \text{ per radian}$$

where subscripts  $o$  again refer to preflight still-air values.

The interested reader can find a comprehensive and detailed discussion of the "free" oscillation technique in reference 11.

## REFERENCES

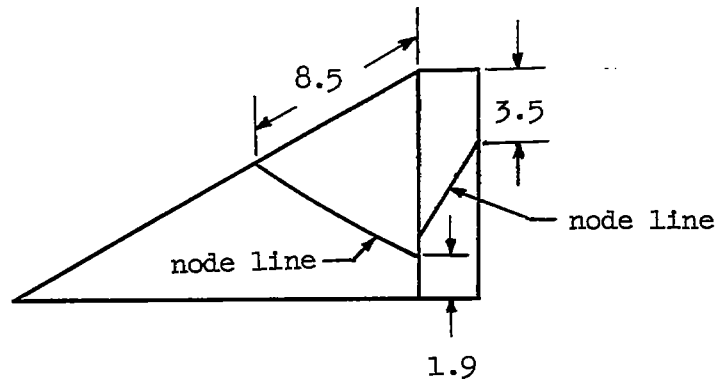
1. Nelson, Herbert C., and Berman, Julian H.: Calculations on the Forces and Moments for an Oscillating Wing-Aileron Combination in Two-Dimensional Potential Flow at Sonic Speed. NACA Rep. 1128, 1953. (Supersedes NACA TN 2590.)
2. Nelson, Herbert C., Rainey, Ruby A., and Watkins, Charles E.: Lift and Moment Coefficients Expanded to the Seventh Power of Frequency for Oscillating Rectangular Wings in Supersonic Flow and Applied to a Specific Flutter Problem. NACA TN 3076, 1954.
3. Erickson, Albert L., and Stephenson, Jack D.: A Suggested Method of Analyzing for Transonic Flutter of Control Surfaces Based on Available Experimental Evidence. NACA RM A7F30, 1947.
4. Henning, Allen B.: Results of a Rocket-Model Investigation of Control-Surface Buzz and Flutter on a 4-Percent-Thick Unswept Wing and on 6-, 9-, and 12-Percent-Thick Swept Wings at Transonic Speeds. NACA RM L53I29, 1953.
5. Reese, David E., Jr.: An Experimental Investigation at Subsonic and Supersonic Speeds of the Torsional Damping Characteristics of a Constant-Chord Control Surface of an Aspect Ratio 2 Triangular Wing. NACA RM A53D27, 1953.
6. Anon.: Tables of Aerodynamic Coefficients for an Oscillating Wing-Flap System in a Subsonic Compressible Flow. Rep. F.151, Nationaal Luchtvaartlaboratorium, Amsterdam, May 1954.
7. Martin, Dennis J., Thompson, Robert F., and Martz, C. William: Exploratory Investigation of the Moments on Oscillating Control Surfaces at Transonic Speeds. NACA RM L55E31b, 1955.
8. Reese, David E., and Carlson, William C. A.: An Experimental Investigation of the Hinge-Moment Characteristics of a Constant-Chord Control Surface Oscillating at High Frequency. NACA RM A55J24, 1955.
9. Thompson, Robert F., and Moseley, William C., Jr.: Oscillating Hinge Moments and Flutter Characteristics of a Flap-Type Control Surface on a 4-Percent-Thick Unswept Wing With Low Aspect Ratio at Transonic Speeds. NACA RM L55K17, 1956.
10. Thompson, Robert F.: Investigation of a 42.7° Sweptback Wing Model To Determine the Effects of Trailing-Edge Thickness on the Aileron Hinge-Moment and Flutter Characteristics at Transonic Speeds. NACA RM L50J06, 1950.

11. Coleman, Robert P.: Damping Formulas and Experimental Values of Damping in Flutter Models. NACA TN 751, 1940.

TABLE I

DYNAMICAL CONSTANTS OF MODELS

	Model A	Model B
Wing first bending (control wing), cps . . . . .	188	-----
Aileron-wing mode (control wing), cps . . . . .	-----	202
(See sketch below)		



Aileron-wing mode.

Wing first bending (no control wing), cps . . . . .	255	180
Control still-air frequency, cps . . . . .	44.4	41.1
No other wing or control modes were apparent from the shake tests up to a frequency of 400 cps.		
Control inertia about hinge line, slug-ft <sup>2</sup> . . . . .	0.000468	0.000756
Control mass unbalance, slug-ft . . . . .	0.00307	0.00474

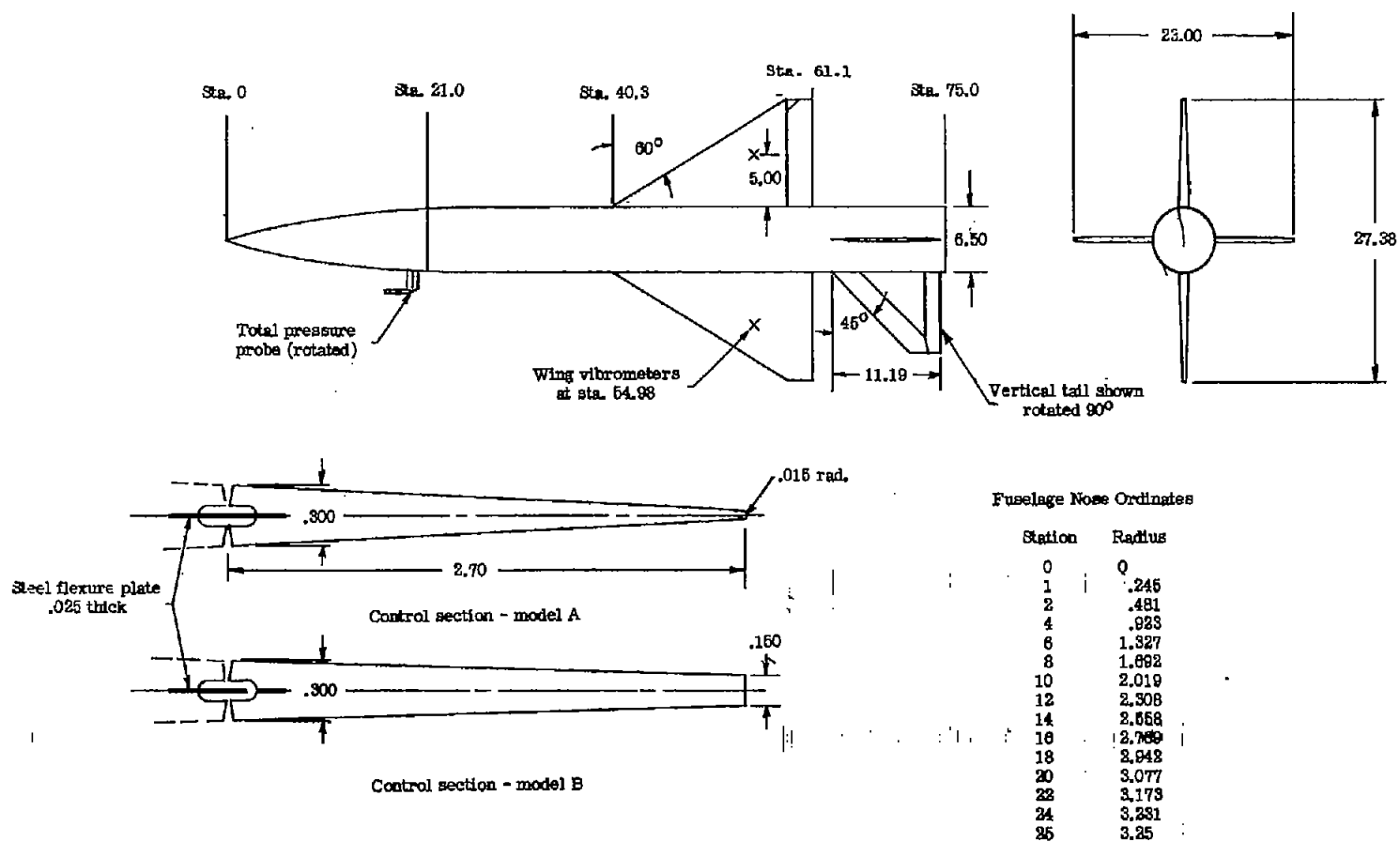
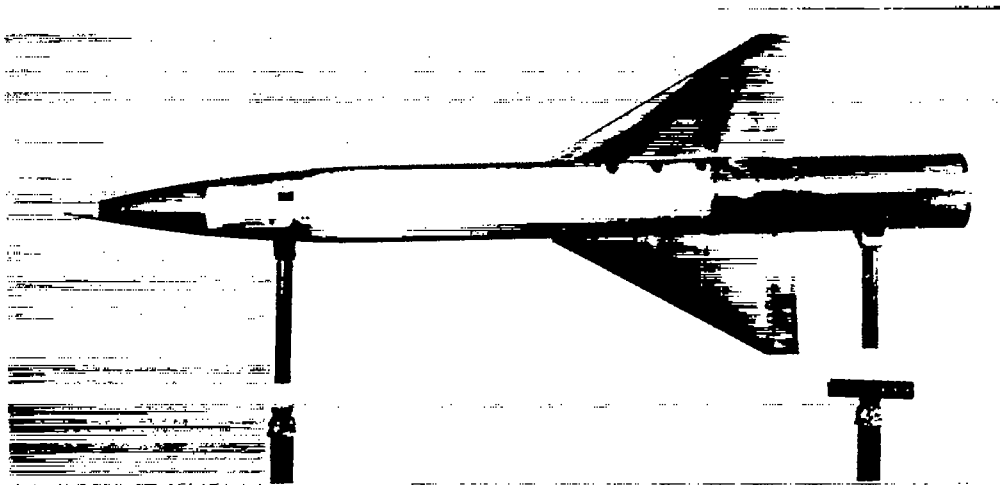
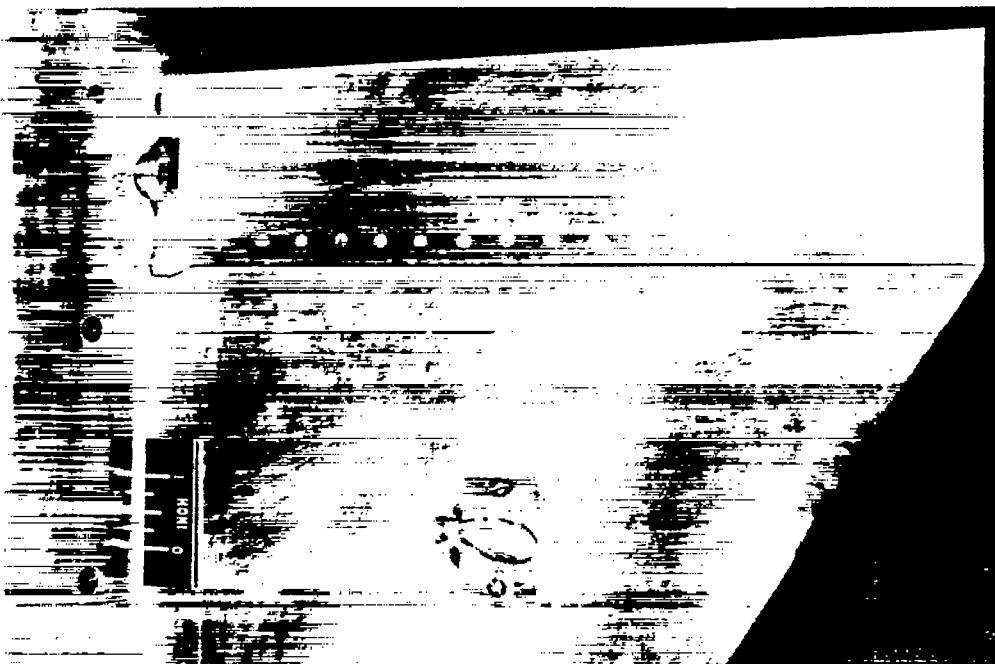


Figure 1.- Details of control damping model. All dimensions are in inches.



(a) Model plan view.

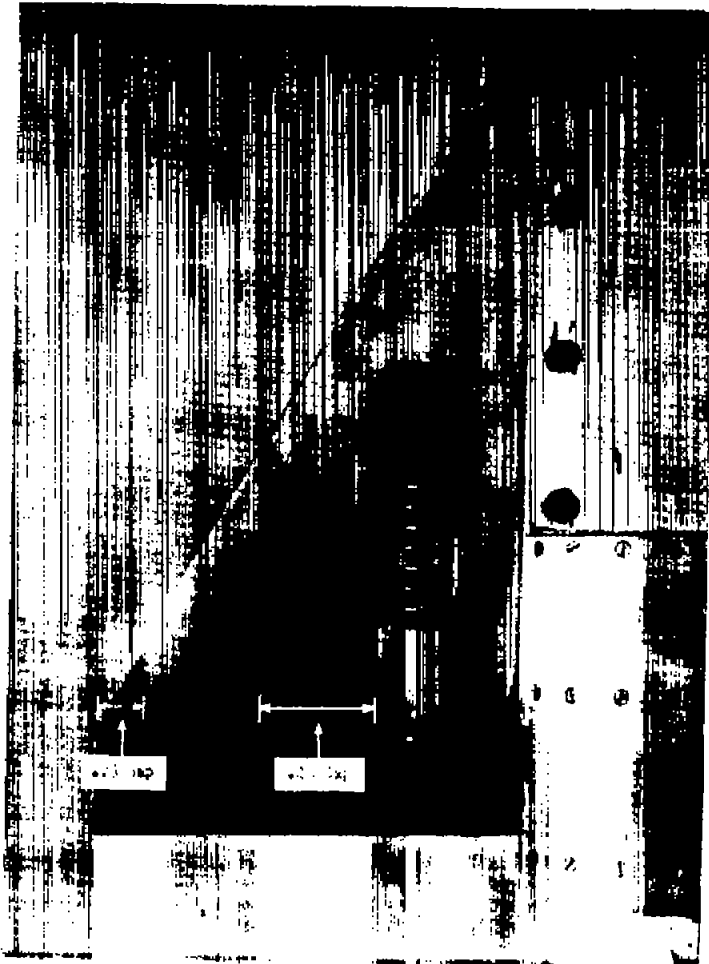
L-87754.1



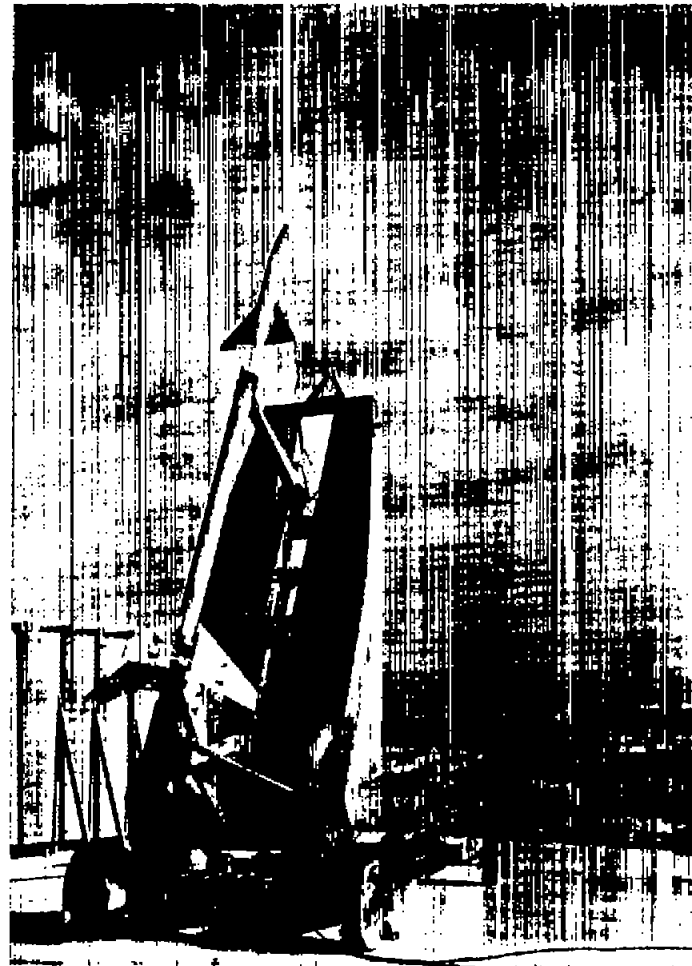
(b) Wing-control close-up; model B.

L-87756

Figure 2.- Model photographs.

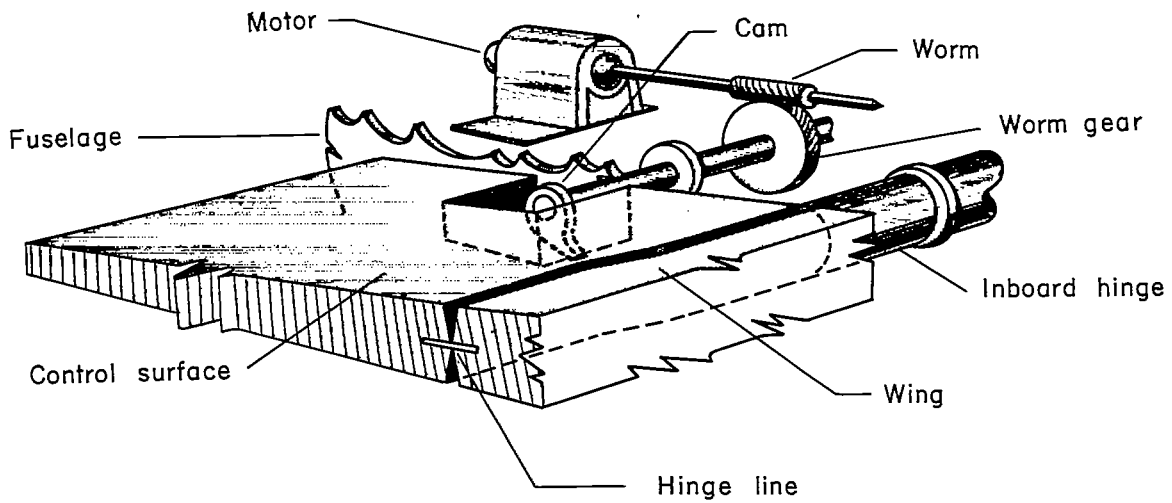


L-91905.1  
(c) Wing-control close-up; model A.

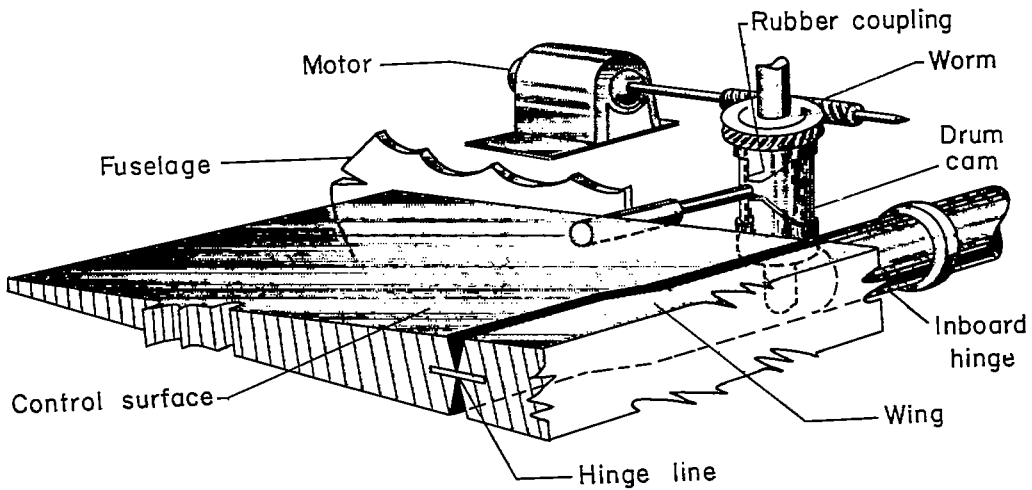


L-91903.1  
(d) Model and booster on launching rig.

Figure 2.- Concluded.



(a) Model B.



(b) Model A.

Figure 3.- Sketch of model plucking systems (not to scale).

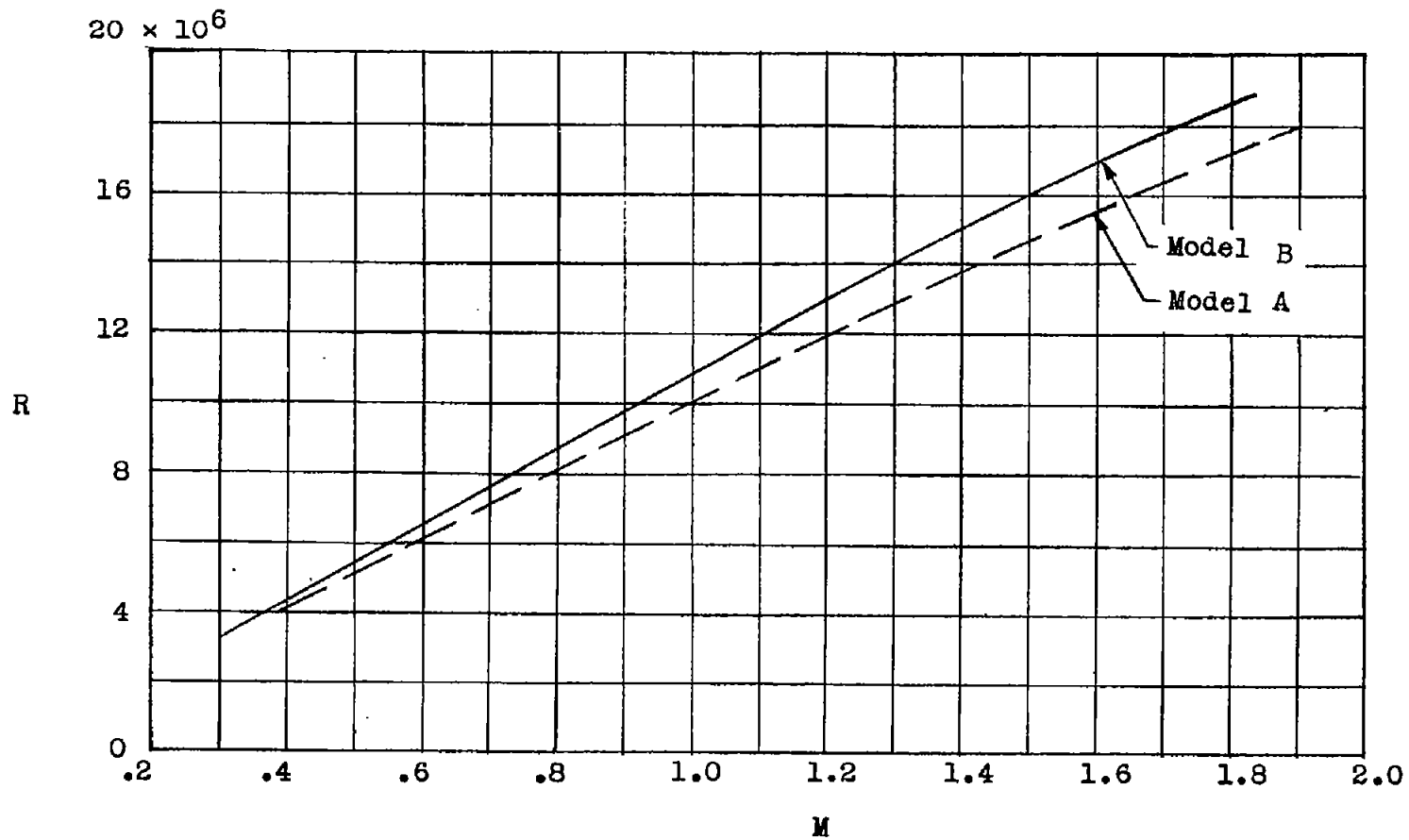


Figure 4.- Variation of Reynolds number with Mach number (accelerated flight).

CONFIDENTIAL

CONFIDENTIAL

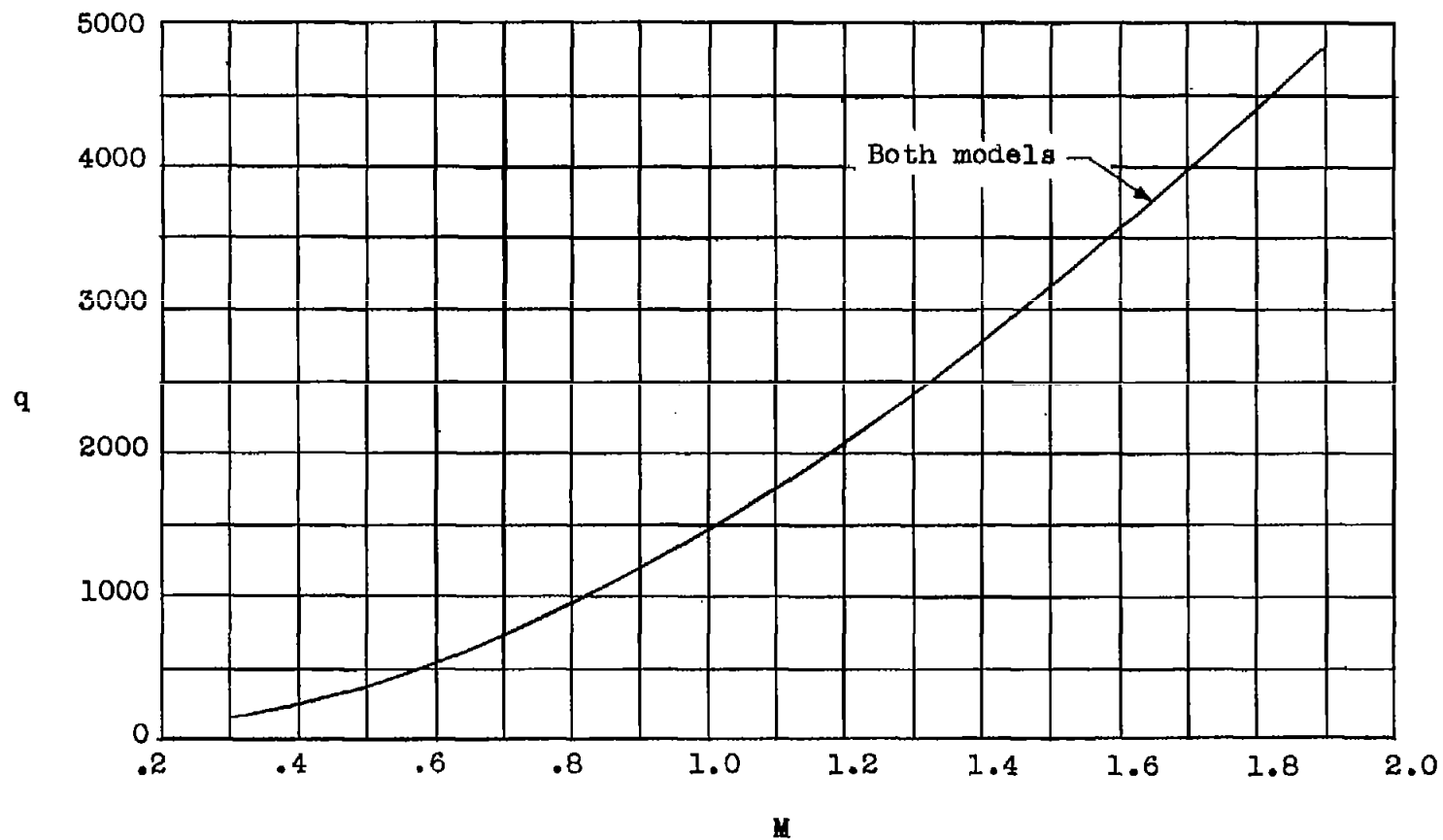
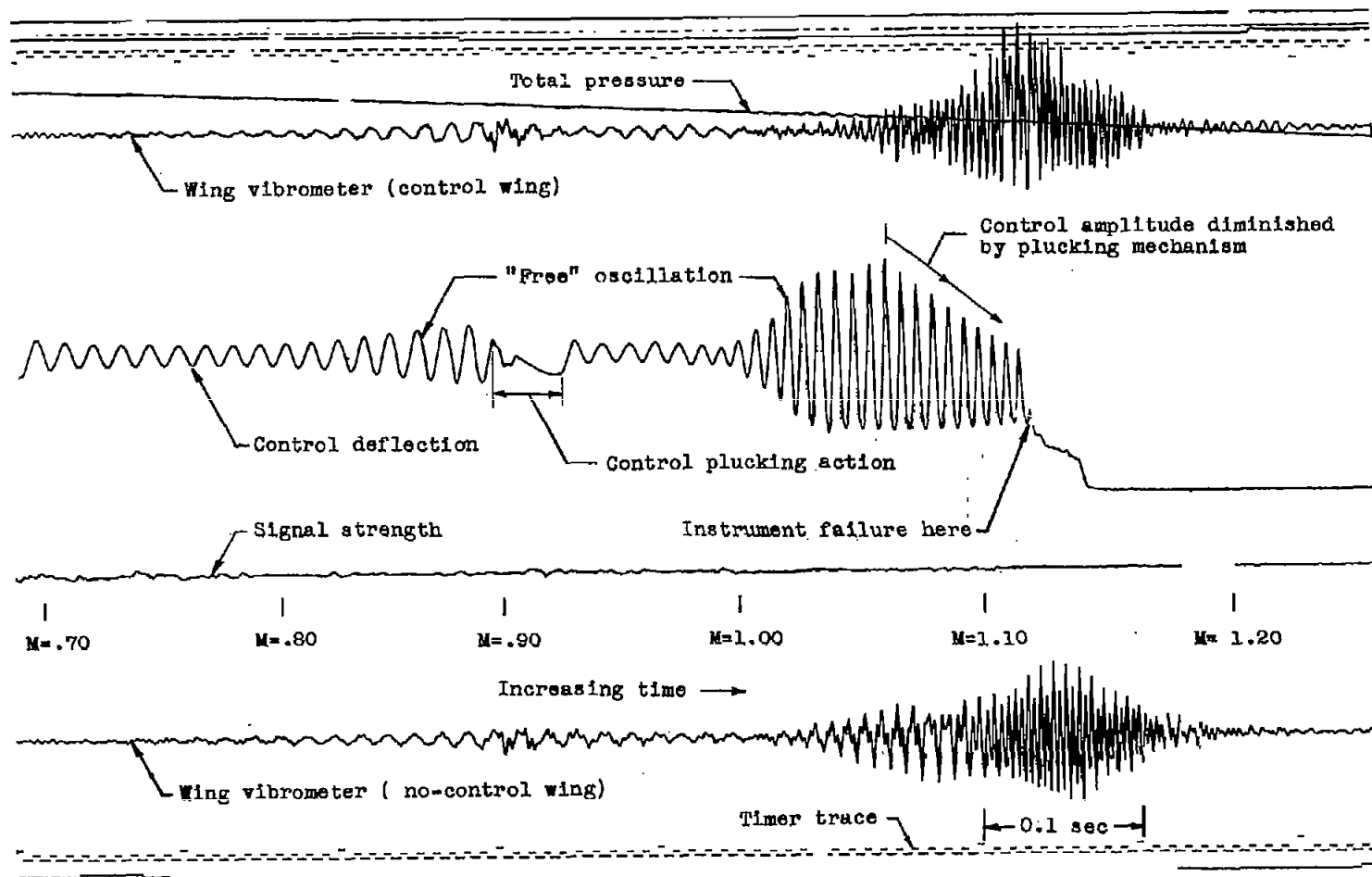
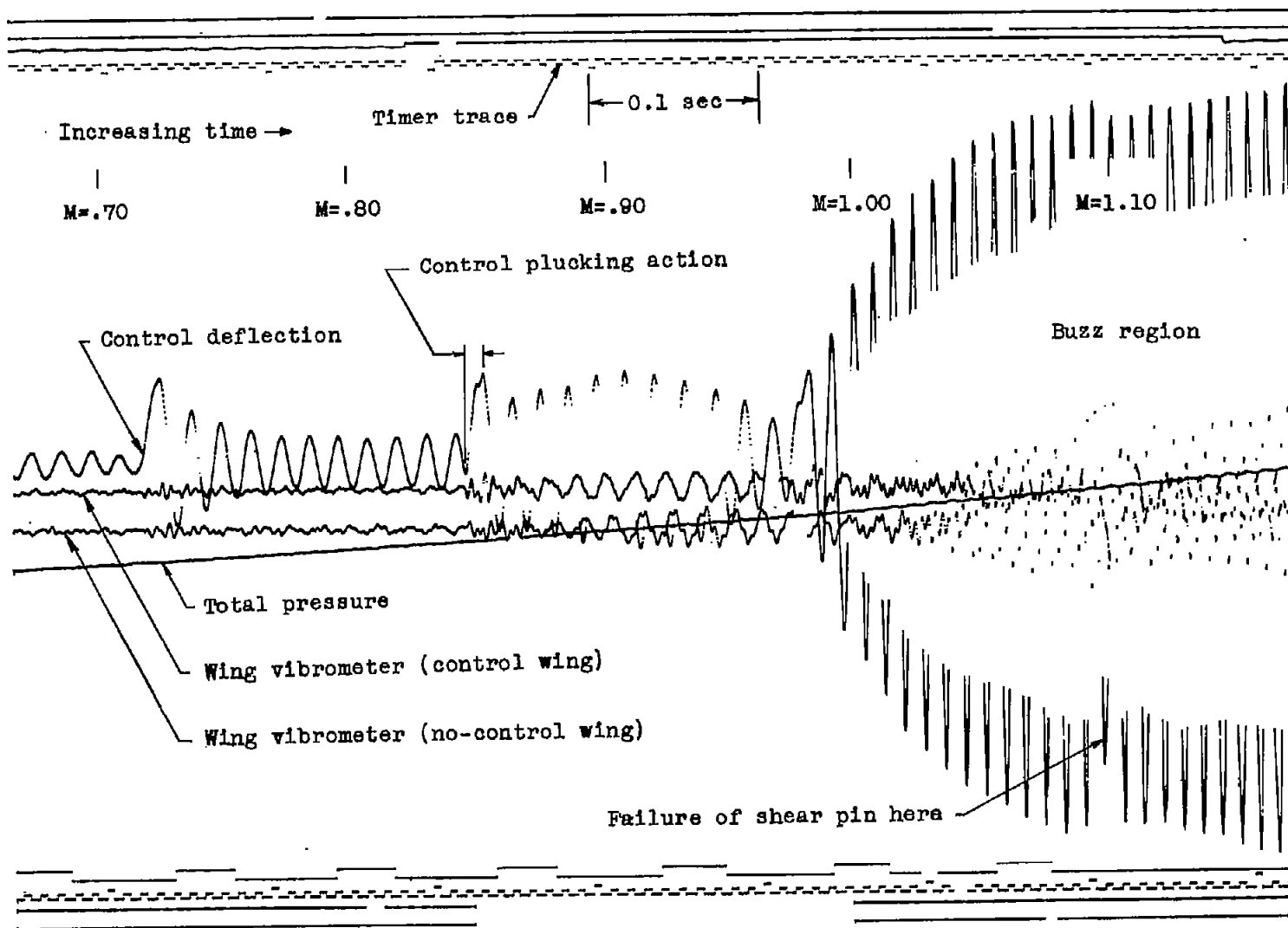


Figure 5.- Variation of dynamic pressure with Mach number (accelerated flight).



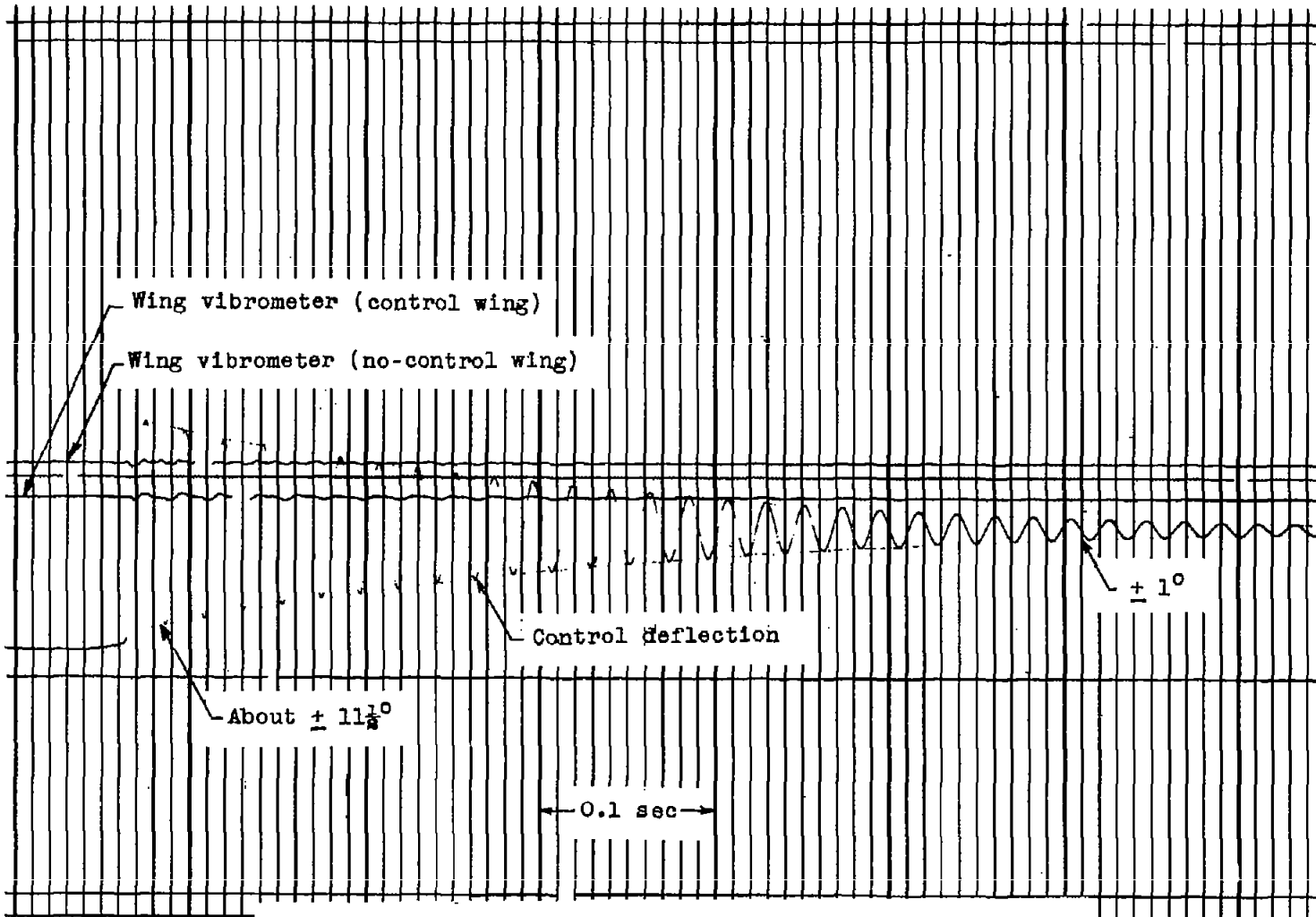
(a) Model A.

Figure 6.- Specimen telemeter records.



(b) Model B.

Figure 6.- Continued.



(c) Still air response of model A control to a step input.

Figure 6.- Concluded.

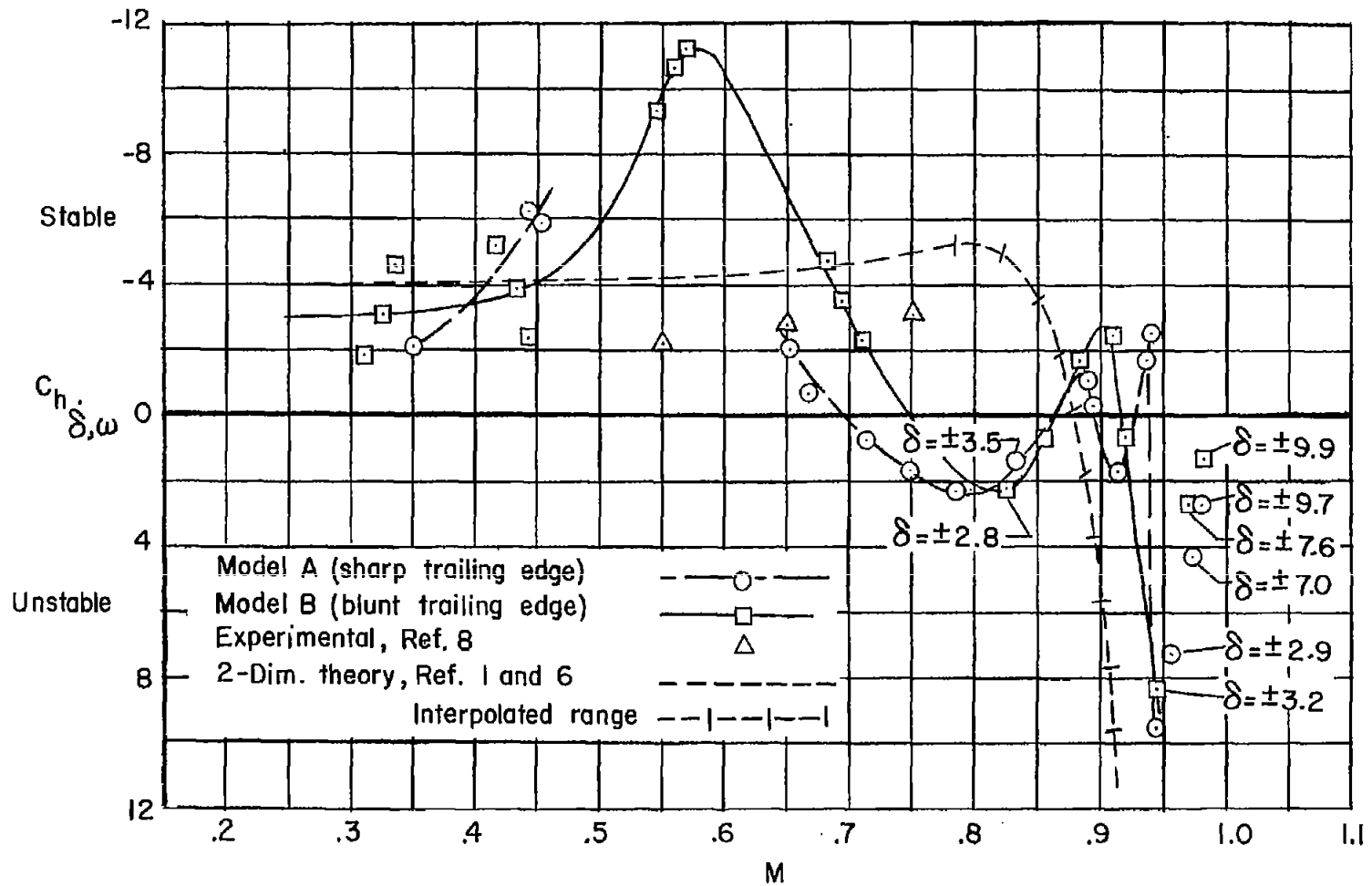


Figure 7.- Effect of Mach number on control damping coefficient. Control oscillation amplitude from  $\pm 1^\circ$  to  $\pm 2\frac{1}{2}^\circ$  except as noted.

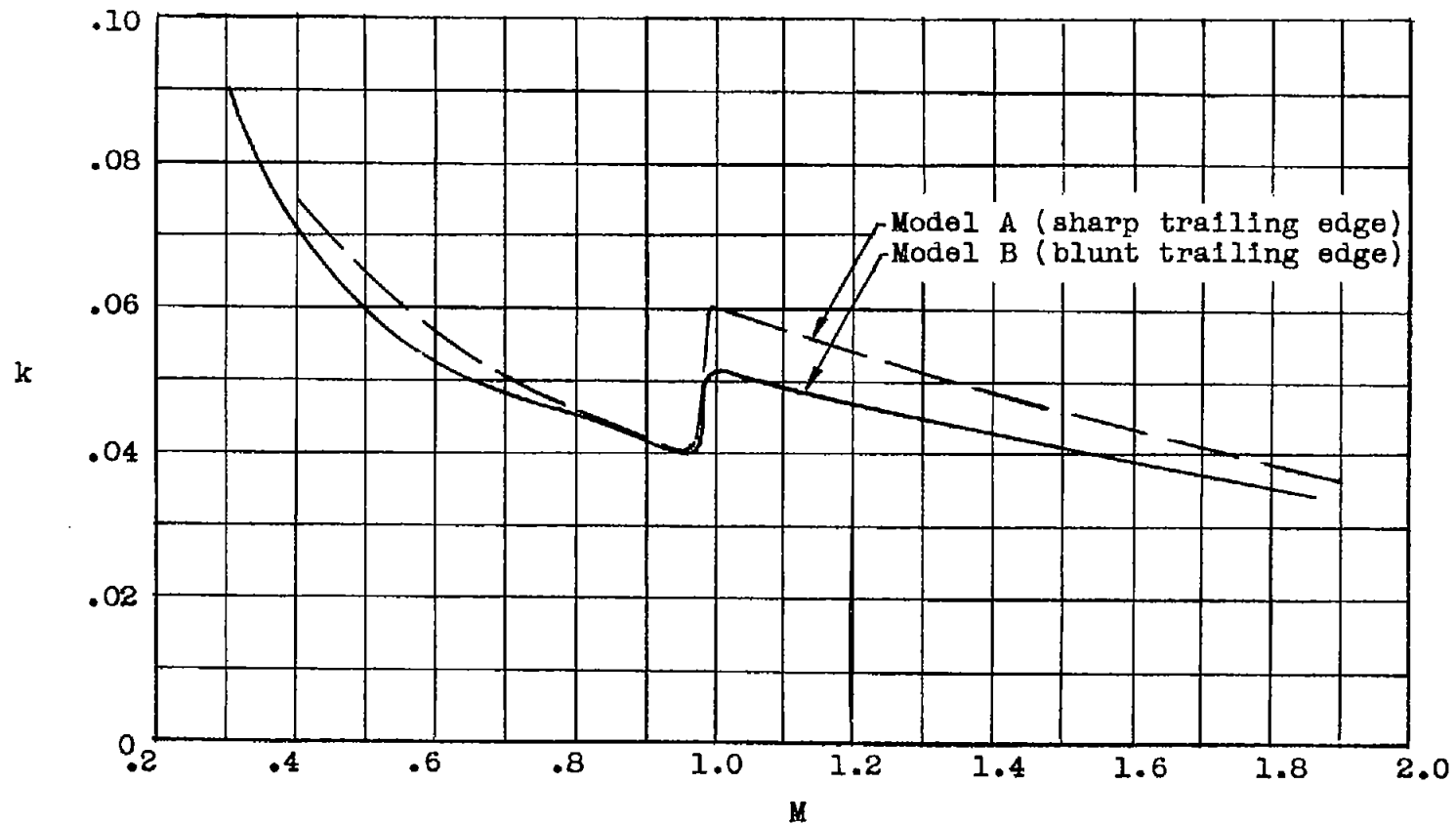


Figure 8.- Variation of reduced frequency with Mach number.

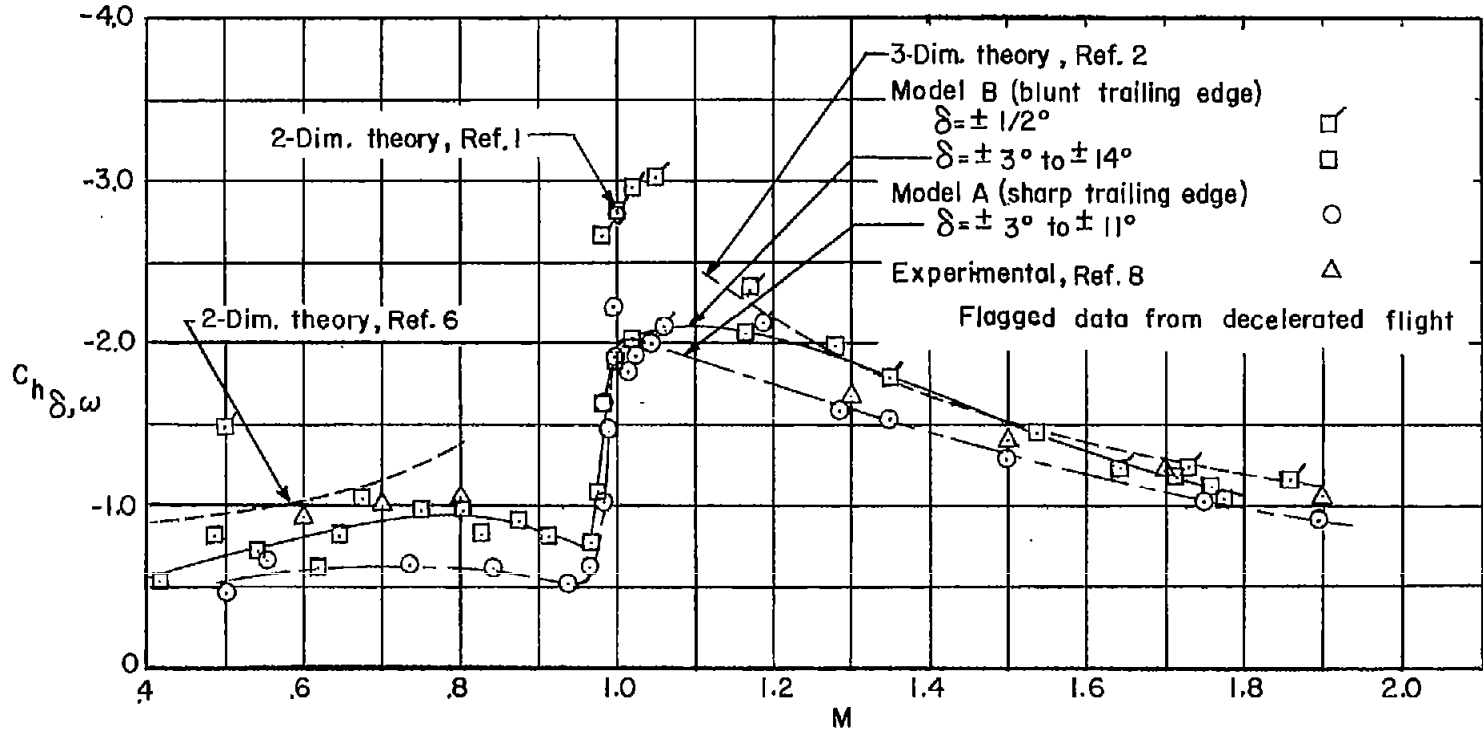


Figure 9.- Variation of control restoring-moment coefficient with Mach number.